SEMPA Studies of Exchange Coupling in Magnetic Multilayers

R.J. Celotta, D.T. Pierce, and J. Unguris

Introduction

In the late 1980s, a number of exciting yet puzzling observations resulted from experiments investigating the coupling between two ferromagnetic layers separated by a nonferromagnetic spacer layer. A pioneering experiment by Grünberg et al.[1] showed that Fe layers separated by a thin Cr spacer aligned with antiparallel magnetization, but with Au as the spacer layer, a parallel alignment occurred. The long-range magnetic dipole from each layer would tend to explain antiparallel alignment; small pinholes in the spacer layer would produce parallel alignment. Alternatively, the layers might be coupled through the spacer-layer conduction electrons by the Ruderman-Kittel-Kasuya-Yosida (RKKY) effect. This was expected to produce an oscillation in coupling as the spacer thickness increased, that is, an oscillation between parallel and antiparallel alignment. Oscillatory coupling was first observed by Parkin et al.[2] Researchers had also found[3,4] that, at spacer thicknesses where antiparallel alignment occurred, the Fe/Cr/Fe system can exhibit a giant magnetoresistance (GMR) effect, that is, an anomalously large change in resistance when a magnetic field is applied. The potential technological importance of the GMR effect to magnetic sensing and magnetic information storage added further impetus to the already rapidly growing area of research in magnetic multilayers.

Subsequent research greatly extended the range of systems studied and also added to the outstanding questions: What determines the period of the oscillation in the coupling? Does it depend in detail on the spacer-layer material, or is it roughly the same for most materials? What role, if any, does the RKKY effect play and could it account for the observed phenomena? Answering these questions proved difficult, largely because meaningful comparisons with theory required layer-by-layer growth with sharp interfaces in a variety of new epitaxial systems. Further, mapping out the systematic variation of coupling with spacer-layer thickness required the production of a series of multilayer systems differing, in an accurately known way, only by the thickness of the spacer layer. We chose to study[5] the problem of these coupled magnetic layers by using scanning electron microscopy with polarization analysis (SEMPA).

The SEMPA Fe/Cr/Fe Experiment

The SEMPA method[6] is an extension of SEM. In a conventional scanning electron microscope, the number of secondary electrons produced by the highly focused probe beam at the surface is taken as a measure of the topography. In SEMPA, the degree of spin polarization of those same secondary electrons provides a measure of the surface magnetization under the probe beam. SEMPA

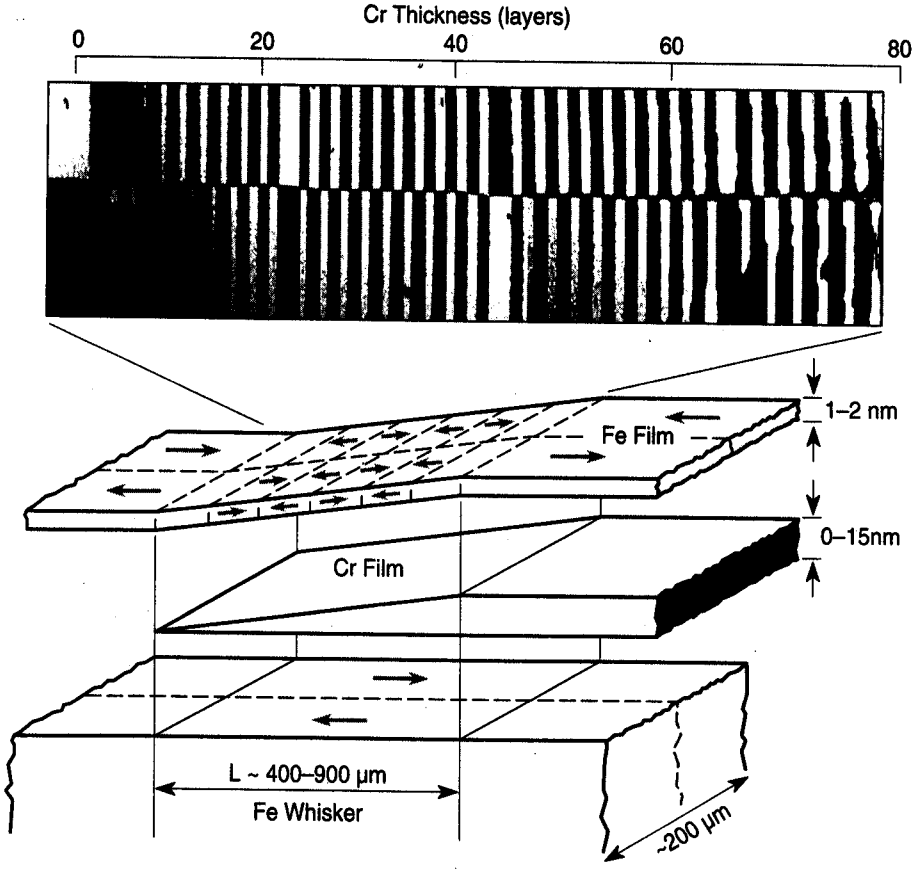

Figure 1. At the bottom, a schematic representation of the fabricated sample showing a single-crystal Fe whisker with two domains, a film of Cr grown in a wedge shape to provide a spacer-layer thickness variation, and an epitaxial overlayer of Fe. The top shows actual SEMPA measurements of the domain structure in the Fe overlayer.

images of the domain structure of magnetic materials can be obtained with a resolution of 20 nm. The intrinsic independence of the structural and magnetic information in SEMPA can be used to study the influence of structure on magnetism.

We studied the Fe/Cr/Fe system, a lattice-matched epitaxial system with smooth interfaces, in an effort to approximate, as nearly as possible, the ideal system envisioned in theory. Important to this selection was the availability[7] of single-crystal Fe whiskers, which have very flat surfaces and are exceptionally free from bulk crystal defects. Chromium provided a spacer material with less than a 0.6% lattice mismatch. We grew the Cr spacer layer in the shape of a wedge so that there would be a continuous variation of spacer-layer thickness, all with the same substrate and grown under the same conditions. The small width of the whiskers (<1 mm) immediately suggested the use of microscopy, but independent of the specimen size, the small surface area needed in a microscopy experiment makes it much easier to find an ideal substrate structure.

In Figure 1, we schematically show the Fe whisker with two oppositely directed domains indicated, running along its length; the Cr wedge spacer layer; and a 1–2 nm Fe overlayer film. The Fe whisker was sputter-cleaned and annealed in a manner demonstrated, via scanning tunneling microscopy (STM) measurements,[9] to produce an atomically perfect substrate with single-monolayer high steps every μm or so. The wedge was produced by slowly uncovering the substrate by scanning a knife edge above the whisker during Cr deposition. At the top of the figure, the SEMPA image of the Fe overlayer dramatically shows the exchange-coupling effect: The white (black) region corresponds to magnetization directed to the right (left). The magnetization direction alternates with each additional atomic Cr layer thickness, except for "phase slips" in the pattern at 24, 44, and 64 layers, extending out to almost 80 monolayers of Cr.

The unprecedented number of oscillations observed is due, in no small part, to the quality of the substrate used and the care taken during the growth process. For example, Figure 2 shows three very different patterns of alternation in magnetization corresponding to three different substrate temperatures during Cr wedge growth. Our STM measurements[10] show that the thickness fluctuations in the Cr spacer layer, owing to roughness induced during growth,

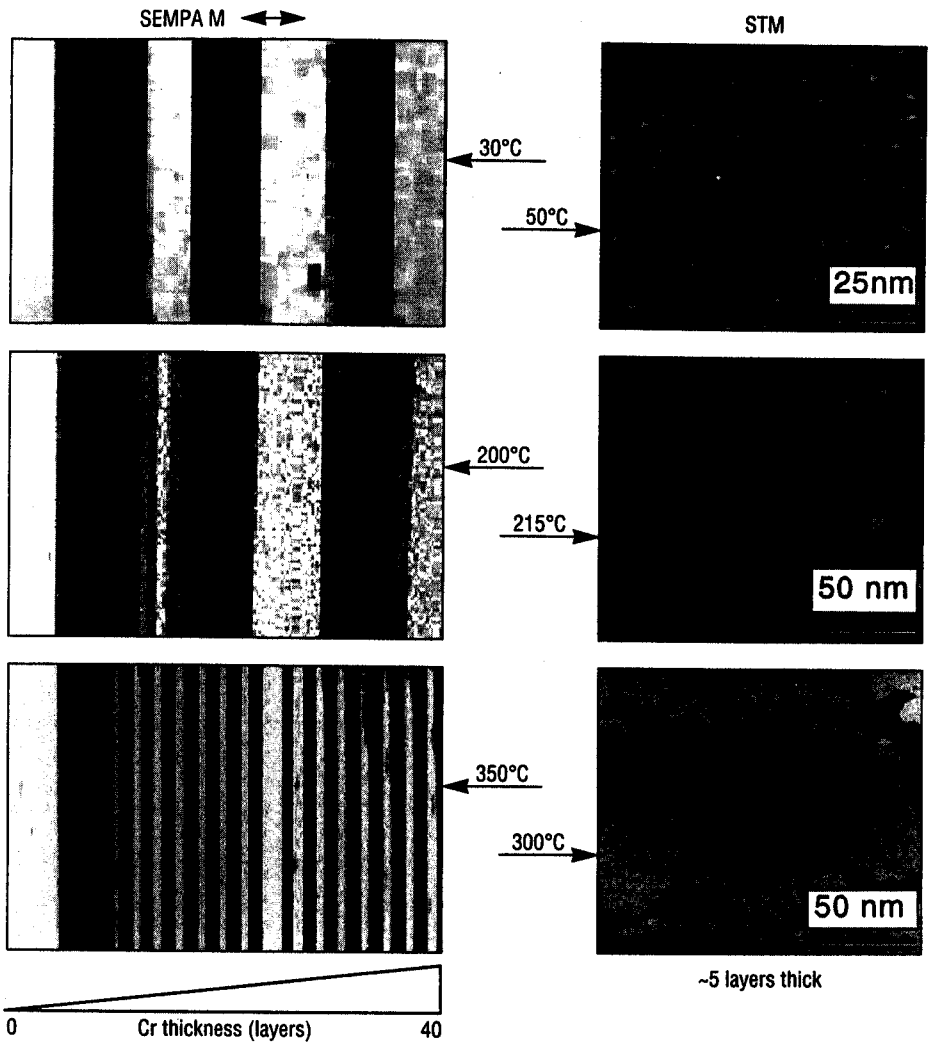

Figure 2. Left: Three SEMPA images of the top-layer Fe magnetization for different substrate temperatures during growth of the Cr wedge. Right: STM topographs for approximately five layers of Cr on Fe for growth conditions similar to those for the SEMPA images to the left, showing the clear correlation between growth and magnetic structure.

determine which of the two discrete oscillation periods is observed. For low-temperature growth, a long-period oscillation is observed; at high temperature, we see the short-period oscillation; and at an intermediate temperature, both may be seen. The bottom STM topograph in Figure 2, for high-temperature growth, exhibits layer-by-layer growth of Cr on the Fe whisker substrate. Under these circumstances, the strong, short-period oscillations in the exchange coupling dominate. Near room temperature, the Cr growth is rougher and the growth front has several unfilled Cr layers open simultaneously; layers three to seven can be seen in the upper STM topograph of a nominally five-layer-thick film. In the corresponding SEMPA image, one might expect to see a complex mosaic of tiny domains in the Fe overlayer, reflecting the reversal in overlayer magnetization with each monolayer difference in Cr layer thickness as implied by the short-period exchange coupling. However, there is a large energy cost associated with the consequential high density of regions of opposing magnetization in the Fe overlayer. These abrupt changes in direction are suppressed because the *intralayer* coupling within the Fe overlayer is stronger than *interlayer* coupling between Fe layers. The fluctuations in the Cr spacer-layer thickness act to low-pass

filter to eliminate the short-period oscillation, and the underlying long-period oscillation becomes visible. This makes clear how subtle changes in growth conditions can lead to different observed periods. This also explains why the same growth technique, applied to a wide variety of elemental systems, might contribute to a "filtering" tendency, resulting in the observation of similar periods independent of material.

Comparisons between experiments or between experiment and theory depend on the ability to *accurately* determine oscillation periods; this is a particular strength of the microscopic approach used here. In the case of good epitaxial growth, the exact number of monolayers deposited is frequently monitored by measuring the oscillations in intensity of a reflection high-energy electron diffraction (RHEED) beam diffracted from the surface while depositing the overlayers. A beam diffracted from islands in the $n + 1$ layer as well as from the uncovered n layer can be made to interfere so as to reduce the RHEED intensity; the intensity returns to its former value when layer $n + 1$ is complete and the interference vanishes. The evolution of islands into layers, as seen by the RHEED beam during deposition, is preserved exactly in the Cr wedge and can be viewed by scanning the RHEED beam along the wedge in the direction of increasing thickness, that is, the elapsed deposition time. Using the SEM beam in a RHEED configuration and measuring the diffracted intensity as the SEM beam rasters over the wedge region produces a RHEED image of the sample, as seen in the top of Figure 3. The alternating white and black lines correspond to interference maxima and minima, and provide a measure of the thickness of the Cr wedge accurate to ±0.1 monolayer over the entire sample. The bottom magnetization image was selected to further illustrate the effects of imperfect growth. Note that in the regions where the RHEED intensity oscillations vanish, owing to a rougher growth mode replacing the layer-by-layer mode, the short-period exchange-coupling oscillation also disappears.

Comparison with Theory

An important goal of this work was to measure the exchange-coupling periods with accuracy sufficient to stringently test any theoretical explanation. The current theoretical understanding[11-13] is based on an RKKY-like indirect exchange interaction mediated by the conduction electrons of the middle layer.

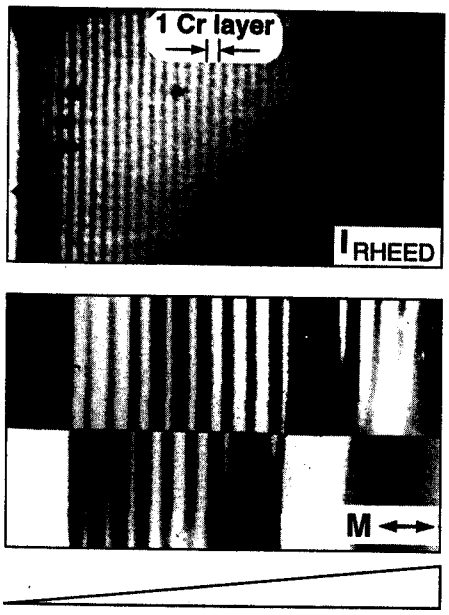

Figure 3. Top: A RHEED image of the Cr wedge in an Fe/Cr/Fe sample before depositing the Fe overlayer, showing RHEED intensity oscillations with Cr thickness. Matching the RHEED and SEMPA images provides a thickness scale accurate to ±0.1 layer. Bottom: The SEMPA magnetization image after deposition of the Fe overlayer. Note the correspondence between the RHEED intensity oscillations, indicating layer-by-layer growth and the short-period oscillations.

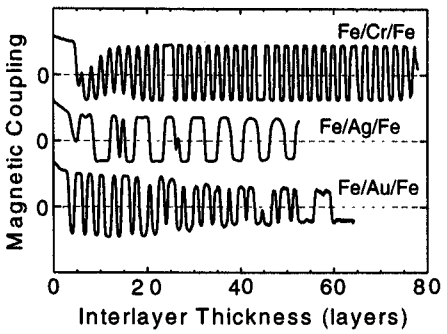

Figure 4. SEMPA line scans of the magnetization along the long axis of the Fe whisker as a function of the thickness of the Cr, Ag, and Au spacer layers. The excellent growth of these systems on the nearly ideal Fe(100) whisker substrate allows the measurement of the exchange coupling over a large range of spacer-layer thickness (>10 nm), allowing very accurate determination of the coupling periods.

The specific periodicity of the coupling is determined by the spacer layer's Fermi surface, or more specifically, by the value of its extremal spanning vectors. Calculations of the expected periods are now available for most of the systems studied experimentally.

The experimental exchange-coupling periods are determined from SEMPA data by reducing the full image to a line trace, showing the modulation in alignment direction as a function of spacer-layer thickness, as shown on the top of Figure 4 for Fe/Cr/Fe. Since SEMPA measures coupling direction but not coupling strength, the number and the exact positions of the zero crossings are of paramount importance. Because of the large number of oscillations observed and the high accuracy of the thickness calibration, we are able to determine[10] the period of the short-period oscillation in Fe/Cr/Fe to be 2.105±0.005 layers, in excellent agreement with the 2.1 layer period, from the appropriate spanning vector calculated for the Cr Fermi surface.[11] The closeness of the period of the exchange-coupling oscillations to the crystal-lattice constant explains the beating effect seen in Figure 1 as a periodic phase slip at 24, 44, and 64 layers of Cr. The short exchange-coupling period is the same as that of the spin-density wave in bulk antiferromagnetic Cr. This is not surprising since both arise from the same strong nesting of the Cr Fermi surface. Interestingly, we can observe the exchange-coupling oscillation well above the Néel temperature of bulk Cr. The Fe substrate can be thought of as inducing a modulation in the spin density of the paramagnetic Cr with a period determined by its Fermi surface. Indeed, the spin polarization of a series of Cr layers on Fe was also measured using SEMPA[14] and shows a spin structure at the Cr surface that alternates with each additional Cr layer. When an Fe layer was subsequently deposited, it aligned itself opposite to the top Cr layer.

While the Fe/Cr/Fe system is rich in complexity, the purpose of confirming that the proposed theoretical explanation is correct is best served by less complicated systems. Hence, similar experiments were made on the Fe/Ag/Fe[15] and Fe/Au/Fe[16] systems, as shown in Figure 4. These systems also offer the possibility of excellent growth. The simpler Fermi surfaces of noble metals, in contrast to transition metals like Cr, give rise to fewer periods that are easier to correlate with the observed coupling periods. The measured modulations exhibited both long- and short-period oscillations

of comparable strength, making accurate (1–3%) determinations of both periods possible.

Conclusions

We have found that accurate determinations of exchange-coupling periods, possible in SEMPA wedge experiments on systems exhibiting excellent epitaxial growth, are in excellent agreement with predictions of the exchange-coupling periods based on the extremal vectors of the spacer-layer Fermi surface. On the basis of this series of experiments and on those of others using a wide variety of techniques, the theoretical underpinning for the origin of exchange-coupling periods in magnetic multilayers is now well-understood. This work proved particularly informative about the crucial role physical structure plays in multilayer magnetism.

Critical to making a useful comparison between observation and prediction was the ability to perform the full experiment within the field of view of a microscope on a nanostructure grown for this specific purpose. This permitted us to use the best available substrate, to select the best region for deposition, and to grow and monitor the epitaxy *in situ*. We were able to measure the subtle changes with layer thickness without the systematic errors that accompany the fabrication of multiple samples. The ability to fabricate nanostructures permits the capture—within a single micrograph—of changes with respect to a selected parameter. This provides us with a powerful new extension of the SEMPA technique.

Although many of the initial questions are now answered, a large number have since arisen. While we now understand the origin of the period of the oscillations, the strength of the coupling remains less well-understood. The SEMPA images also exhibit biquadratic coupling, that is, the film magnetization is coupled at right angles where the normal (bilinear) coupling is weak, and this is not fully understood. Finally, subtle anomalies in the magnetic and physical structure at the Fe-Cr interface have been observed that demand further investigation. We expect that the techniques described here, with suitable modifications, will continue to prove useful in answering these new questions.

Acknowledgments

The authors wish to acknowledge many fruitful discussions with M.D. Stiles and J.A. Stroscio. We also thank J.A. Stroscio for providing the STM topographs. This work was supported in part by the Office of Naval Research.

References

1. P. Grünberg, R. Schreiber, Y. Pang, M.B. Brodsky, and H. Sowers, *Phys. Rev. Lett.* **57** (1986) p. 2442.
2. S.S.P. Parkin, N. More, and K.P. Roche, *ibid.* **64** (1990) p. 2304.
3. M.N. Baibich, J.M. Broto, A. Fert, F. Nguyen Van Dau, F. Petroff, P. Etienne, G. Creuzet, A. Friederich, and J. Chazelas, *ibid.* **61** (1988) p. 2472.
4. G. Binasch, P. Grünberg, F. Saurenbach, and W. Zinn, *Phys. Rev. B* **39** (1989) p. 4828.
5. D.T. Pierce, J. Unguris, and R.J. Celotta, in *Ultrathin Magnetic Structures II*, edited by B. Heinrich and J.A.C. Bland (Springer-Verlag, Berlin, 1994) p. 117.
6. M.R. Scheinfein, J. Unguris, M.H. Kelley, D.T. Pierce, and R.J. Celotta, *Rev. Sci. Instrum.* **61** (1990) p. 2501.
7. Fe whiskers were provided by Simon Fraser University under an operating grant from the National Science and Engineering Research Council of Canada.
8. J. Unguris, R.J. Celotta, and D.T. Pierce, *Phys. Rev. Lett.* **67** (1) (1991) p. 140.
9. J.A. Stroscio, D.T. Pierce, and R.A. Dragoset, *ibid.* **70** (1993) p. 3615.
10. D.T. Pierce, J.A. Stroscio, J. Unguris, and R.J. Celotta, *Phys. Rev. B* **49** (1994) p. 14,564.
11. P. Bruno and L. Chappert, *Phys. Rev. Lett.* **67** (1991) p. 1602.
12. M.D. Stiles, *Phys. Rev. B* **48** (1993) p. 7238.
13. K.B. Hathaway, in *Ultrathin Magnetic Structures II*, edited by B. Heinrich and J.A.C. Bland (Springer-Verlag, Berlin, 1994), p. 45–81, and references therein.
14. J. Unguris, R.J. Celotta, and D.T. Pierce, *Phys. Rev. Lett.* **69** (1992) p. 1125.
15. J. Unguris, R.J. Celotta, and D.T. Pierce, *J. Magn. Mat.* **127** (1993) p. 205.
16. J. Unguris, R.J. Celotta, and D.T. Pierce, *J. Appl. Phys.* **75** (1994) p. 6437. □